Preparation of N-doped ZnO-loaded halloysite nanotubes catalysts with high solar-light photocatalytic activity

Zhi-Lin Cheng and Wei Sun

ABSTRACT

N-doped ZnO nanoparticles were successfully assembled into hollow halloysite nanotubes (HNTs) by using the impregnation method. The catalysts based on N-doped ZnO-loaded HNTs nanocomposites (N-doped ZnO/HNTs) were characterized by X-ray diffraction (XRD), transmission electron microscopy-energy dispersive X-ray (TEM-EDX), scanning electron microscopy-energy dispersive X-ray (SEM-EDX), UV-vis and Fourier transform infrared spectroscopy (FT-IR) techniques. The XRD pattern showed ZnO nanoparticles with hexagonal structure loaded on HNTs. The TEM-EDX analysis indicated ZnO particles with the crystal size of ca.10 nm scattered in hollow structure of HNTs, and furthermore the concentration of N atom in nanocomposites was up to 2.31%. The SEM-EDX verified most of N-ZnO nanoparticles existing in hollow nanotubes of HNTs. Besides containing an obvious ultraviolet absorbance band, the UV-vis spectra of the N-doped ZnO/HNTs catalysts showed an available visible absorbance band by comparing to HNTs and non-doped ZnO/HNTs. The photocatalytic activity of the N-doped ZnO/HNTs catalysts was evaluated by the degradation of methyl orange (MO) solution with the concentration of 20 mg/L under the simulated solar-light irradiation. The result showed that the N-doped ZnO/HNTs catalyst exhibited a desirable solar-light photocatalytic activity.

Key words | clay, halloysite nanotubes, N-doped ZnO, photocatalysis

Zhi-Lin Cheng (corresponding author)
Wei Sun
College of Chemistry and Chemical Engineering,
Yangzhou University,
225002,
China
E-mail: *zlcheng224@126.com*

INTRODUCTION

Owing to its wide band gap (3.3 eV) and large excitation binding energy of 60 meV, ZnO has gained more and more attention in the field of environmental purification for its high catalytic activity, low cost and environmental friendliness (Kityk *et al.* 2002). However, optical absorption in the ultraviolet region deters the wide scale use of ZnO for photocatalytic activities under sunlight. Many studies reported on improvement of visible-light photocatalytic activity of metal oxide semiconductors by doping metals (Motshekga *et al.* 2013), non-metals (Nian *et al.* 2009), and surface modification (Rajbongshi *et al.* 2014a, b). Nitrogen has been regarded as the most-promising acceptor dopant because of its low ionization energy, suitable ionic radius, ease of handling, low material toxicity, and source abundance, and therefore is widely used to increase visible light absorption by modifying the band gap (Yu *et al.* 2013). So far, many synthesized studies of N-doped ZnO as photocatalysis have been reported (Lim *et al.* 2007; Li *et al.* 2011; Naouara *et al.* 2014). These results showed that the properties of N-doped metal oxide depend on the synthesis method and employing nitrogen sources. The different types of techniques have been used to prepare N-doped ZnO nanocomposites including implementation, sputtering and treatment in nitrogen-containing atmosphere at high temperature (Lee *et al.* 2005; Game *et al.* 2012). To achieve pre-concentration of pollutants and improve the separation of nanosized active particles, immobilization of active particles on an adsorbent or an inert support to create integrated photocatalytic adsorbents (IPAs) has been proposed (Shan *et al.* 2010). Using IPAs, degradation of pollutants can be achieved by the simultaneous effects of physical adsorption by the adsorbent and photochemical degradation by the immobilized ZnO. To achieve this, ZnO particles are typically dispersed on inert and high surface area supports such as activated carbon (Basha *et al.* 2011), zeolite (Haque *et al.* 2005; Liu *et al.* 2014) and so on.

Several studies have demonstrated that halloysite nanotubes (HNTs) have been of great interest in applications as nanomaterials in different fields. Owing to their inherent

doi: 10.2166/wst.2015.403

hollow nanotube structure and different outside and inside chemistry, HNTs as two-layered aluminosilicate clay have exhibited promising results as a catalyst support (Zhai *et al.* 2010). Compared to carbon nanotubes (CNTs), HNTs as a type of economically available raw materials have some unique characteristics (Wang *et al.* 2010). More recently, the synthesis of carbon-coated HNTs (CCH) via the carbonization of sucrose-coated HNTs in the presence of sulfuric acid has been reported (Zhang *et al.* 2014). Metal oxide (MO) nanoparticles (ZnO, TiO_2) were subsequently deposited on the surface of the CCH to produce MO/CCH nanocomposites. So far, the study on N-doped ZnO particles loaded on HNTs has never been performed.

In this study, we have successfully synthesized the N-doped ZnO-loaded HNTs catalysts by using the impregnation method. The structure of the catalysts was analyzed by X-ray diffraction (XRD), transmission electron microscopy-energy dispersive X-ray (TEM-EDX), scanning electron microscopy-energy dispersive X-ray (SEM-EDX), Fourier transform infrared spectroscopy (FT-IR) and UV-vis characterizations. The photocatalytic activity of the N-doped ZnO-loaded HNTs was evaluated by degradation of methyl orange (MO) under simulated solar-light irradiation.

MATERIALS AND METHOD

Material synthesis

The HNT mineral powder as clay mineral was purchased from Tianjin Linruide Co., Ltd in China. Firstly, 20 g of HNT powder was dried in oven at 120 °C before use. Next, the saturated solution of $Zn(NO_3)_2$ was prepared at room temperature, and then added into an amount of urea to prepare the transparently mixed solution. Then, the above mixed solution was not dropwisely added into hot HNT powder rapidly taken out from oven until the surface of HNT powder was moist. The moist powder above was transferred into the oven and treated at 120 °C for 6 h. Finally, the sample above was calcined at 500 °C for 3 h. The resulted sample was marked as N-doped ZnO/HNTs. Compared to the conventional impregnation-loaded method, the present work improved the impregnation-loaded procedure by adding urea, which was both the N doping source and the precipitating agent for preventing Zn ionic from shifting on external surface of HNTs. In other cases, the non-doped ZnO-loaded HNTs without employing urea were prepared by the above procedures. The preparation process of the impregnation-loaded method is illustrated in Figure 1.

Material characterization

The formation of nanocomposites was confirmed by XRD using a Bruker-AXS D8 Advance powder diffractometer, with operation condition at 40 kV and 30 mA. The morphology and element analysis of sample were observed by TEM-EDX analysis (Tecnai 12, Philips Company). The surface morphology and element analysis of sample was examined by SEM-EDX analysis (S4800II, Hitachi) at an acceleration voltage of 15 kV. IR spectra was recorded in Bruker Sendor 27, with operation condition in the mid-infrared range of the instrument (400–4,000 cm^{-1}) for samples dispersed in KBr pellets in 1:99 ratios. The UV-vis light absorption spectrum was obtained from a Varian Cary 5000 spectrophotometer equipped with an integrating sphere assembly. The FT-IR spectrum was analyzed by a Varian IFS66/S spectrometer. The chemical oxygen demand (COD) value of MO solution was detected by rapid determination instrument (5B-1) and the total organic carbon (TOC) value was measured by TOC-V_{CPH} instrument (Shimadzu company).

Photocatalytic activity

The photocatalytic activity of the prepared material was studied by using probe pollutants of MO under simulated solar-light irradiation flux (source: Xenon lamp, PLS-SXE300, 300W, 200–2,500 nm in the wavelength band). The adsorption–desorption equilibrium was established by keeping the catalyst loaded dye in the dark under stirring with the speed of 60 r/min for one hour. The spectral response of the centrifuged sample solution was recorded by UV-vis spectrophotometer (Lambda 850, PE Company). The initial

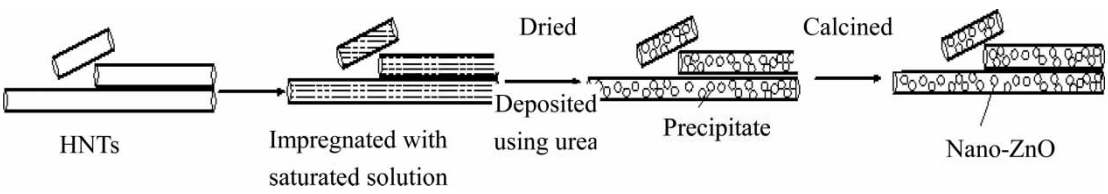

Figure 1 | Preparation illustration of N-doped ZnO/HNTs.

concentration of MO was 20 mg/L. The prepared N-doped ZnO/HNTs catalysts (10 g) were dispersed in 30 L MO aqueous solution by mechanical stirring for 15 min. The photocatalytic activity testing was carried out under stirring with the speed of 60 r/min. Furthermore, the degradation or the removal values in subsequent data all have subtracted the absorption value of HNTs to MO.

RESULTS AND DISCUSSION

Characterization of N-doped ZnO/HNTs

Figure 2 shows the XRD pattern of HNTs and N-doped ZnO/HNTs catalysts. For pure HNTs sample, all of the observed peaks can mainly be indexed to the characteristic peaks of halloysite as shown in Figure 1-HNTs (Wang *et al.* 2010). But for the N-doped ZnO/HNTs catalyst, it is clearly observed that ZnO particles have a hexagonal structure (JCPDF: 891397). No significant peak for nitrogen is observed in N-doped ZnO which suggests the possibility of introduction of nitrogen into the ZnO lattice without affecting the ZnO crystal structure. According to the broadened peaks of the ZnO, the average particle size of the ZnO particles as evaluated by the Scherrer formula is 12.5 nm (Tomita & Sato 2004).

Figure 3 displays the TEM- EDX images of the N-doped ZnO/HNTs catalysts. From the TEM image, it can be observed that the ZnO nanoparticles were successfully assembled into hollow nanotubes of HNTs and the crystal size is about 10 nm (see Figures 3(c) and (d) higher magnification), which is close to the value calculated from the Scherrer formula. Most importantly, besides the peaks of Zn as well as the composition elements of HNTs in EDX spectrum (Figure 3(b)), there appears the N peak.

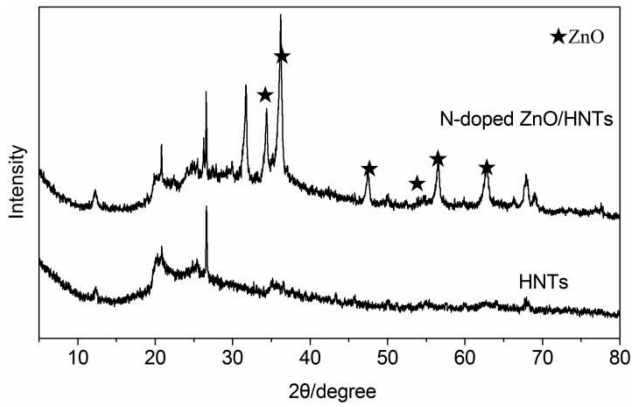

Figure 2 | XRD pattern of HNTs and N-doped ZnO/HNTs.

Table 1 lists the element content of the N-doped-ZnO/HNTs composition analyzed by EDX. The N content in total composition is up to 2.31%. This is likely to confirm that the N-doped ZnO/HNTs catalysts contain a certain concentration of doping N atom, which is ascribed to be a result of the N element doped into the crystal lattice of ZnO. For comparing to the assembled effect of nanoparticles, the outer morphology of the N-doped ZnO/HNTs is shown in SEM-EDX images (see Figure 4). Neither the independent particles on the outer surface of nanotubes nor the energy spectrum peaks of Zn is observed in SEM-EDX images, verifying that most of the ZnO nanoparticles are mainly dispersed in hollow nanotubes of HNTs.

The FT-IR spectra of HNTs and the N-doped ZnO/HNTs catalysts are used to investigate the composition and structure of the resultant samples. As shown in Figure 5, the N-doped ZnO/HNTs possess some signals due to HNTs, such as the deformation of Al-O-Si and Si-O-Si at 536 and 462 cm^{-1}, respectively, and the O-H groups of the inner hydroxyl groups at 909 cm^{-1} as well as Si-O broad stretching band at about 1010 cm^{-1}. By comparing with HNTs, no other characteristic signals are detected on the N-doped ZnO/HNTs. This reason should be attributed to be because most of the N-doped ZnO nanoparticles exist in hollow nanotubes of HNTs. Thus it can be seen that this work developed a high-effective and facile method to assemble the active nanoparticles into the hollow nanotubes of HNTs.

The UV-vis spectra of HNTs, the non-doped ZnO/HNTs and the N-doped ZnO/HNTs catalysts are shown in Figure 6. In contrast to HNTs, the non-doped ZnO/HNTs and N-doped ZnO/HNTs catalysts appear as an obvious absorption band in the UV region of between 300 nm and 400 nm, which is attributed to the typical UV absorption feature of ZnO. Beside it, there is a significant absorption tail band on the visible region of between 400 nm and 600 nm on the spectrum of the N-doped ZnO/HNTs catalysts, which is the typical visible absorption feature of N-doped ZnO (Rajbongshi *et al.* 2014a, b). It suggests that the N element has been successfully doped into the crystal structure of ZnO loaded on HNTs, and thus the N-doped ZnO/HNTs catalysts are available for the visible-light photocatalytic activity.

Photocatalytic activity of HNTs, the non-doped ZnO/HNTs and N-doped ZnO/HNTs catalysts

Figure 7 shows the degradation of 30 L MO solution on HNTs, the non-doped ZnO/HNTs and N-doped ZnO/HNTs catalysts under simulated solar-light irradiation. After keeping pristine HNTs dispersed in MO solution in

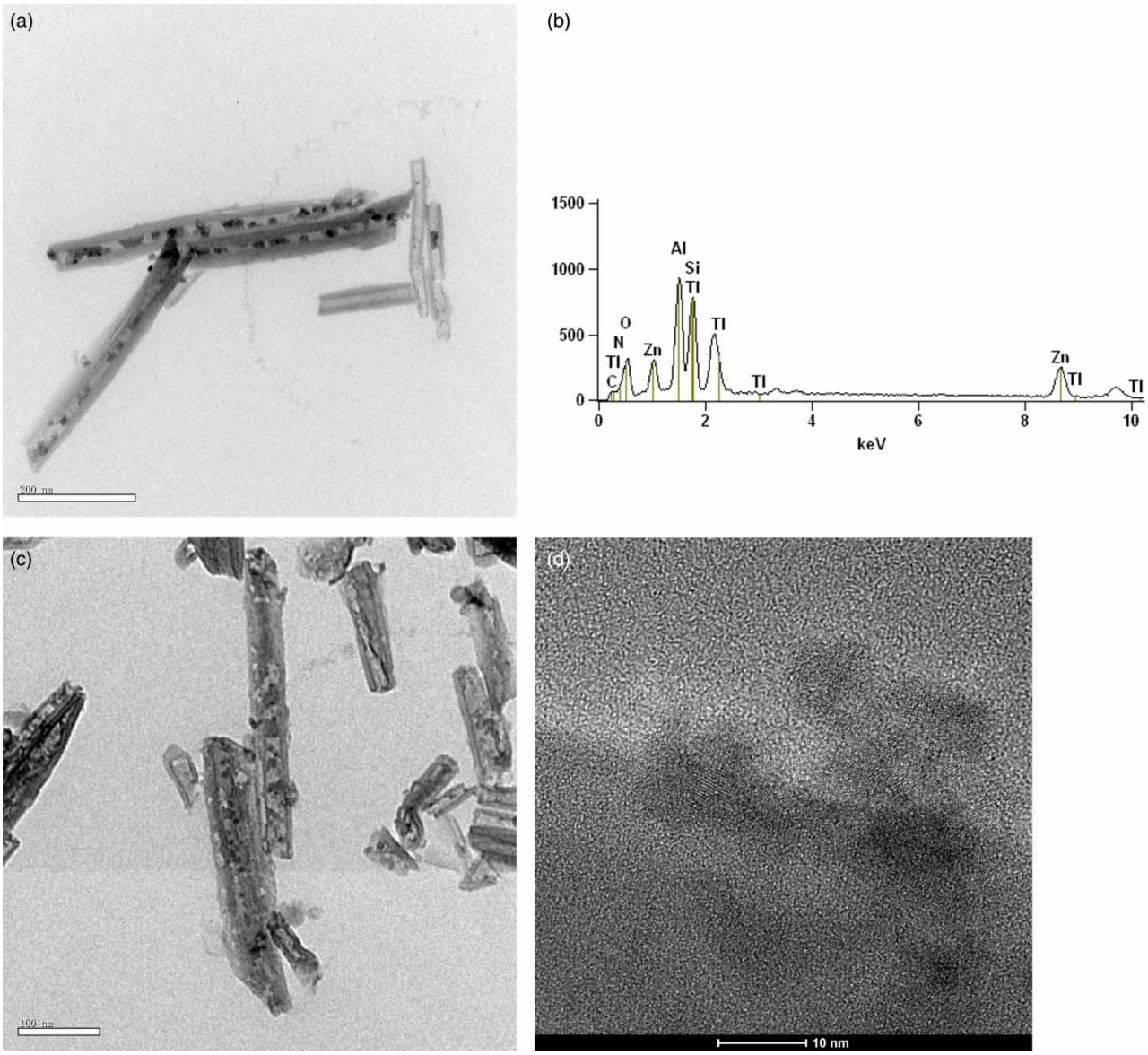

Figure 3 | TEM-EDX images of N-doped ZnO/HNTs: (a) TEM; (b) EDX; (c) and (d) higher magnification.

Table 1 | The EDX analysis of N-doped-ZnO/HNTs composition

	C	N	O	Al	Si	Zn	Ti
Atom%	13.21	2.31	29.65	13.13	22.21	18.99	0.49

the dark for one hour, the concentration of MO solution decreases about 9%, which should be ascribed to the absorption of MO on the porous HNTs. Although then the concentration of MO solution over HNTs has a slight decrease of 10% after starting light source for 30 min of irradiation time, the degradation rate of MO over HNTs hardly changes for further prolonging irradiation time.

Compared to HNTs, the non-doped ZnO/HNTs catalysts exhibit a certain photocatalytic activity for MO. After 480 min of irradiation time, the maximum degradation rate reaches 28%, which is close to three times higher than that of HNTs. Surprisingly, the N-doped ZnO/HNTs catalysts put up a remarkably higher photocatalytic activity for degradation of MO after starting light source for half hour, reaching 30%. As prolonging the irradiation time, the degradation rate of MO is quickly increased before 120 min of irradiation time, and afterwards slightly slowed. This is the reason that the higher concentration of MO prior to 120 min is beneficial to exert the photocatalytic efficiency

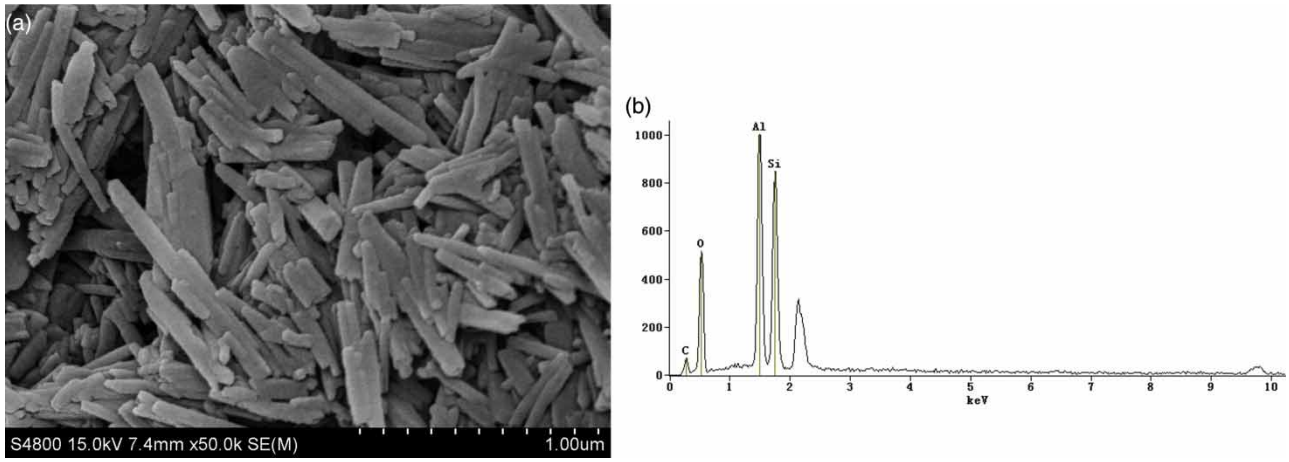

Figure 4 | SEM-EDX images of N-doped ZnO/HNTs: (a) SEM; (b) EDX.

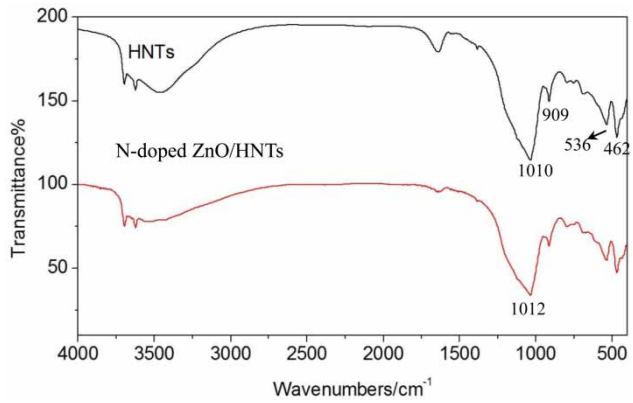

Figure 5 | FT-IR spectra of HNTs and N-doped ZnO/HNTs.

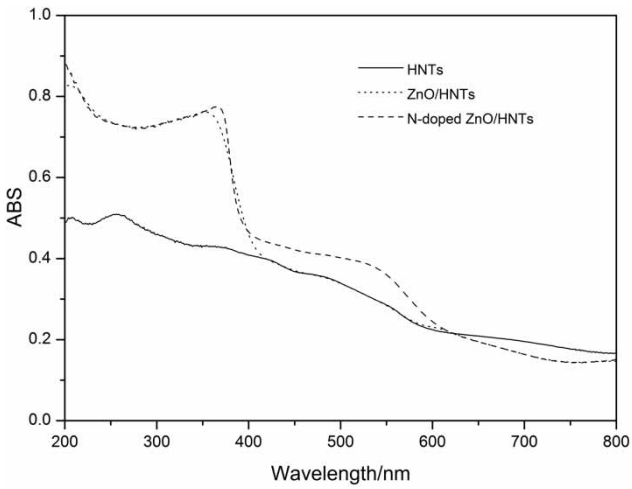

Figure 6 | UV-vis spectra of HNTs, ZnO/HNTs and N-doped ZnO/HNTs.

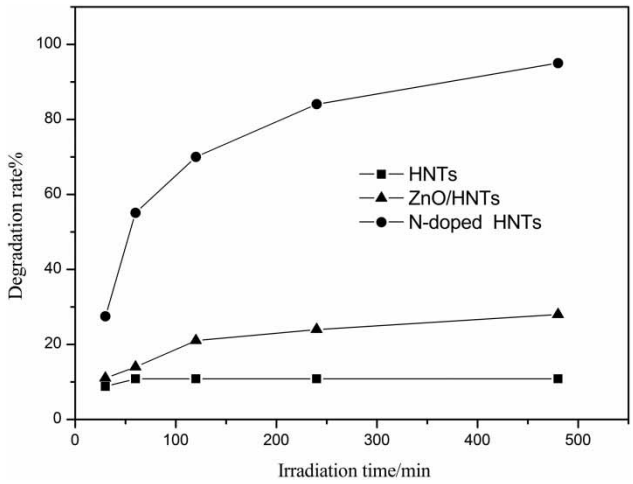

Figure 7 | The degradation rate of MO for HNTs, ZnO/HNTs and N-doped ZnO/HNTs.

of N-doped ZnO. As shown in Figure 7, the degradation rate of MO over the N-doped ZnO/HNTs catalysts reaches 70% after 120 min of irradiation time, which is seven times and 3.5 times higher than those of HNTs and ZnO/HNTs, respectively. The maximum degradation rate of MO over the N-doped ZnO/HNTs catalysts is up to 95%, exhibiting an excellent solar-light photocatalytic activity. Figure 8 shows the UV-vis absorption spectra of MO over HNTs and the N-doped ZnO/HNTs catalysts after different irradiation times. As easily observed, the typical UV-vis absorption peak of MO is between 350 nm and 550 nm in UV-vis spectra. In contrast to MO, the height of the UV-vis characteristic absorption peak of MO solution treated by HNTs with 480 min of solar-light irradiation time

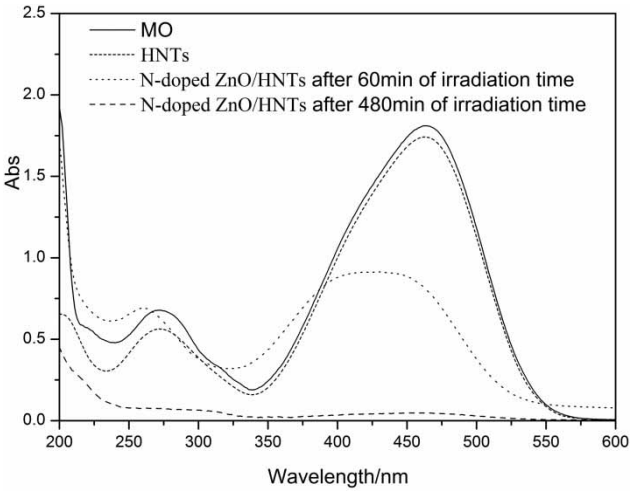

Figure 8 | UV-vis absorption spectra of degradation of MO over HNTs and N-doped ZnO/HNTs.

slightly decreases about 10%, which is close to the absorption value above. However, after MO solution dealt with by the N-doped ZnO/HNTs catalysts with 60 min of irradiation time, the height of the typical UV-vis absorption peak of MO almost decreases about 50%. Upon further extending irradiation time to 480 min, the absorption bands of MO have nearly disappeared. These results are consistent with the degradation rate above. The excellent photocatalytic activity of the N-doped ZnO/HNTs catalysts may be ascribed to the combination effect of the N-doped ZnO nanoparticles and porous HNTs support as adsorbent, i.e. integrated photocatalytic adsorbents (IPAs). Table 2 lists comparison of the degradation rate employing spectrophotography, the COD and TOC removal rate on different irradiation times. It can be found that the COD removal rate is very close to the degradation rate, somewhat lower about 3% than that of the degradation rate. However, the TOC removal rates are remarkably lower about 30% than those of another two methods. These results illustrate that most of MO over N-doped ZnO/HNTs catalysts was decomposed into CO_2 and H_2O relying on photocatalysis, whereas a portion of MO molecular was likely to be converted into other organic molecular inferred by TOC removal value.

Table 2 | Comparison of degradation rates obtained respectively by spectrophotography, COD removal rate and TOC removal rate

Irradiation time (min)	Degradation rate (%)	COD removal rate (%)	TOC removal rate (%)
60	55.1	51.5	23.8
120	70.0	68.8	38.9
480	95.0	92.3	63.1

The high activity of N-doped ZnO is mainly attributed to formation of defects states of N-ZnO nanoparticles due to N-doping (Haque *et al.* 2005). Most importantly, for achieving pre-concentration of pollutants and resolving the separation matter of ZnO nanoparticles, the immobilization of ZnO active nanoparticles on HNTs nanomaterials to create novel integrated photocatalytic adsorbents is more promising for practical application in the removal of harmful organic compounds in wastewater.

CONCLUSIONS

The N-doped ZnO/HNTs catalysts have successfully been prepared by using the impregnation method and urea as N-doping source. The N-doped ZnO/HNTs catalysts showed the high photocatalytic activity for MO degradation under solar-light irradiation.

ACKNOWLEDGEMENTS

This work was supported by the Talent Introduction Fund of Yangzhou University, Jiangsu Social Development Project (BE2014613) and Six Talent Peaks of Jiangsu province (2014-XCL-013). The authors also acknowledge the Project Funded by the Priority Academic Program Development of Jiangsu Higher Education Institutions. The data of this paper originated from the Test Center of Yangzhou University.

REFERENCES

Basha, S., Barr, C., Keane, D., Nolan, K., Morrissey, A., Oelgemöller, M. & Tobin, J. M. 2011 On the adsorption/photodegradation of amoxicillin in aqueous solutions by an integrated photocatalytic adsorbent (IPCA): experimental studies and kinetics analysis. *Photochem. Photobiol. Sci.* **10**, 1014–1022.

Game, O., Singh, U., Gupta, A. A., Suryawanshi, A., Banpurkar, A. & Ogale, S. 2012 Concurrent synthetic control of dopant (nitrogen) and defect complex esto realize broad- band (UV–650 nm) absorption in ZnO nanorods for superior photo-electrochemical performance. *J. Mater Chem.* **22**, 17302–17310.

Haque, F., Vaisman, E., Langford, C. H. & Kantzas, A. 2005 Preparation and performance of integrated photocatalyst adsorbent (IPCA) employed to degrade model organic

compounds in synthetic wastewater. *J. Photochem. Photobiol. A: Chem.* **169**, 21–27.

Kityk, I. V., Ebothe, J., Elchichou, A., Addou, M., Bougrine, A. & Sahraoui, B. 2002 Linear electro-optics effect in ZnO–F film–glass interface. *Phys. Status Solidi(b)* **234**, 553–562.

Lee, S. H., Li, X., Asher, S. E., Coutts, T. J. & Perkins, C. L. 2005 Identification of nitrogen chemical states in N-doped ZnO via X-ray photoelectron spectroscopy. *J. Appl. Phys.* **297**, 034907-1-3.

Li, Z., Sun, S., Xu, X., Zheng, B. & Meng, A. 2011 Photocatalytic activity and DFT calculations on electronic structure of N-doped ZnO/Ag nanocomposites. *Catal. Commun.* **12**, 890–894.

Lim, S. J., Kwon, S. J. & Kim, H. 2007 High performance thin film transistor with low temperature atomic layer deposition nitrogen-doped ZnO. *Appl. Phys. Lett.* **91**, 183517.

Liu, S., Lim, M. & Amal, R. 2014 TiO_2-coated natural zeolite: rapid humic acid adsorption and effective photocatalytic regeneration, *Chem. Eng. Sci.* **105**, 46–52.

Motshekga, S. C., Ray, S. S., Onyango, M. S. & Momba, M. N. B. 2013 Microwave-assisted synthesis, characterization and antibacterial activity of Ag/ZnO nanoparticles supported bentonite clay *J. Hazard. Mater.* **262**, 439–446.

Naouara, M., Ka, I., Gaidi, M., Alawadhi, H., Bessais, B. & Khakani, M. A. E. 2014 Growth, structural and optoelectronic properties tuning of nitrogen-doped ZnO thin films synthesized by means of reactive pulsed laser deposition. *Mater. Res. Bull.* **257**, 47–51.

Nian, H., Hahn, S. H., Koo, K.-K., Shin, E. W. & Kim, E. J. 2009 Sol-gel derived N-doped ZnO thin films. *Mater. Lett.* **63**, 2246–2248.

Rajbongshi, B. M., Ramchiary, A. & Samdarshi, S. K. 2014a Synthesis and characterization of plasmonic visible active Ag/ZnO photocatalyst. *J. Mater. Sci.: Mater. Electron.* **25**, 2969–2973.

Rajbongshi, B. M., Ramchiary, A. & Samdarshi, S. K. 2014b Influence of N-doping on photocatalytic activity of ZnO nanoparticles under visible light irradiation. *Mater. Lett.* **134**, 111–114.

Shan, A. Y., Ghazi, T. I. M. & Rashid, S. A. 2010 Immobilisation of titanium dioxide onto supporting materials in heterogeneous photocatalysis: A review. *Appl. Cat. A: Gen.* **389**, 1–8.

Tomita, A. & Sato, T. 2004 Luminescence channels of manganese-doped spinel. *J. Lumin.* **109**, 19–24.

Wang, J. H., Zhang, X., Zhang, B., Zhao, Y. F., Zhai, R., Liu, J. D. & Chen, R. F. 2010 Rapid adsorption of Cr (VI) on modified halloysite nanotubes. *Desalination* **259**, 22–28.

Yu, Z., Yin, L. C., Xie, Y., Liu, G., Ma, X. & Cheng, H. M. 2013 Crystallinity-dependent substitutional nitrogen doping in ZnO and its improved visible light photocatalytic activity. *J. Colloid Interface Sci.* **400**, 18–23.

Zhai, R., Zhang, B., Liu, L., Xie, Y. D., Zhang, H. Q. & Liu, J. D. 2010 Immobilization of enzyme biocatalyst on natural halloysite nanotubes. *Catal. Commun.* **12**, 259–263.

Zhang, Y., Yang, J. O. & Yang, H. M. 2014 Metal oxide nanoparticles deposited onto carbon-coated halloysite nanotubes. *Applied Clay Science* **95**, 252–259.

First received 2 February 2015; accepted in revised form 20 July 2015. Available online 3 August 2015